2010 21st International Lightning Detection Conference
19 – 20 April • Orlando, Florida, USA
3rd International Lightning Meteorology Conference
21 – 22 April • Orlando, Florida, USA

# A METHOD TO IDENTIFY THE BETTER WRF PARAMETERIZATIONS SET TO DESCRIBE LIGHTNING OCCURRENCE

Zepka, G. S.; Pinto Jr., O.
*National Institute for Space Research* – INPE, São José dos Campos, SP, Brazil

## 1. INTRODUCTION

Numerical Weather Prediction (NWP) model outputs result from computer integrations of the equations governing the physical processes that occur in the atmosphere. NWP output is never a perfect forecast of real atmosphere variables for several reasons: the knowledge of the mathematical formulations of the physics is incomplete; assumptions and short-cuts have been made in the mathematical formulation of models due to computer-time limitations; the knowledge of initial conditions of the variables is restricted because they must be sampled at a finite number of points in space; there are computer round-off errors in the integrations; and it is widely believed from predictability theory that the maximum period in which detailed predictions of atmospheric flow will have any accuracy is about two weeks (Stanski et al, 1989).

In the NWP models it is possible to distinguish a dynamic core, which is responsible for the proper formulation of the equations along with the techniques employed in solving them, and a set of parameterizations representing all those phenomena that are not fully resolved by the dynamic core. These physical processes that cannot in practice be represented by the hydrodynamics laws in its basic form due to their microscopic and discontinuous nature are called subgrid scale processes. The parameterizations schemes consist of simplified alternatives formulas in place of complex theoretical models to resolve the terms associated with the momentum, heat and humidity turbulence fluxes that appear in consequence of the equations integration.

The Weather Research and Forecasting (WRF) Model (Skamarock et al., 2005) is a next-generation mesoscale numerical weather prediction system designed to serve both operational forecasting and atmospheric research needs. It is a fully compressible, non-hydrostatic atmospheric model that uses a terrain-following hydrostatic-pressure vertical coordinate. The effort to develop WRF has been a collaborative partnership, principally among the National Center for Atmospheric Research (NCAR), the National Oceanic and Atmospheric Administration (NOAA), the National Centers for Environmental Prediction (NCEP), the Forecast Systems Laboratory (FSL), the Air Force Weather Agency (AFWA), the Naval Research Laboratory, the University of Oklahoma and the Federal Aviation Administration (FAA). WRF allows researchers the ability to conduct simulations reflecting either real data or idealized configurations. WRF provides operational forecasting to a model that is flexible and efficient computationally, while offering the advances in physics, numeric and data assimilation contributed by the research community.

WRF is used by many operational services for short and medium range weather forecasting and is also an accessible research tool, as it offers multiple physics options that can be flexibly combined in many ways. The model physics parameterizations are categorized in a modular way, as follows: *microphysics*, *cumulus parameterizations*, *surface physics*, *planetary boundary layer physics* and *atmospheric radiation physics* (Skamarock et al., 2005). There are many interactions among these schemes via the model state variables (potential temperature, moisture, wind, etc.) and their tendencies, and via the surface fluxes.

In face of this broad availability of parameterizations it is difficult to define what combination better describes a meteorological phenomenon, application or interest region. Since there is almost no documentation about WRF parameterizations performance over South America, some studies address this question from different perspectives. Ruiz et al. (2007) and Ruiz and Saulo (2006) analyze the WRF sensitivity to the use of different planetary boundary layer and convective parameterizations. These works sought the best model configuration to short and medium range forecasts focusing on rain representation and the

potential impact of planetary boundary layer. The effects of these combinations over other variables were not studied. Ruiz et al. (2009) discussed the possibility to find an optimum configuration of WRF parameterizations for operational purposes over South America. Results showed that the sensitivity of short range weather forecasts to different choices in the model physics is large, but none of the combinations considered has shown significantly better results over the whole model domain. Silva Júnior (2009) evaluated the sensibility of the planetary boundary layer parameterization in the simulation of photochemical pollutants above the Metropolitan Region of São Paulo, by using the WRF model with the coupling of chemical modules (WRF/Chem).

In the present paper, a method to identify which is the combination of parameterizations in WRF model that better represents the atmospheric conditions when lightning occurs in the Brazil southeastern is proposed. It is well known that the primary conditions for the storm formation are the atmospheric thermal profile, moisture and upward movement. Therefore the common parameters used for forecasting thunderstorms and the potential for lightning mostly rely on stability and thermodynamical indexes. In this way, short range simulations of variables of interest for days with lightning were run using three different sets of physical options.

In order to check the consistency and quality of WRF model runs against a corresponding observation of what actually occurred or some good estimate of the true outcome, it is presented also a case study of the day with the highest number of cloud-to-ground (CG) lightning flashes from whole study period.

## 2. LIGHTNING DATA

CG lightning flashes data from the Brazilian Lightning Detection Network (BrasilDat) from October 2005 to March 2006 were used in this study. Pinto Jr. et al. (2006) presented a comparative analysis of the mean monthly distributions of the number of CG flashes, the percentage of positive CG flashes and the peak current of negative and positive CG flashes observed in Brazil for the period from 1999 to 2004, with the same distributions observed by similar networks in other countries (United States, Austria, Italy and Spain) for long time periods (seven to ten years). It was found that the period of large lightning activity throughout the year in Brazil is from October to March due mostly to the increase in the number of storms caused by the spring and summer differential warming.

The region of interest (Figure 1) covers part of the Brazil southeastern including almost all the São Paulo state, the south of Minas Gerais state and the northeast extreme of Paraná state. This area is purposely coincident with the WRF nested domain that will be presented in the next section.

Only those days with more than 300 CG lightning flashes in ± 10 minutes close by the full hours of the afternoon (17 to 21 UT) were selected for this study, totalizing a 38-day dataset. Naccarato (2006) showed the lightning activity peaks in the afternoon (following the daily cycle of insolation) nearby 18-19 UT studying the diurnal variation of the CG lightning flashes for 6 years (1999-2004) in the Brazil southeastern. At this time necessary conditions to instability in the atmosphere are generated and there is greater availability of energy for convection (Iribarne and Cho, 1980).

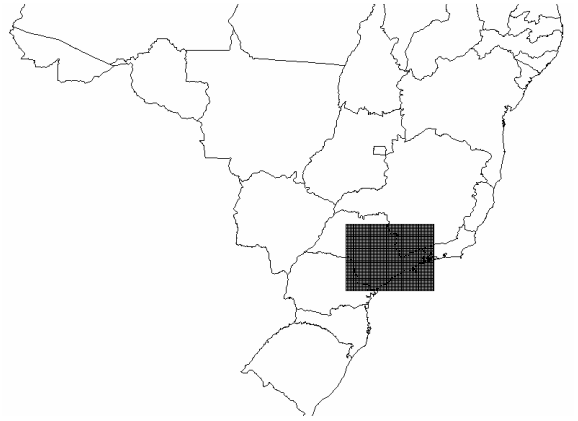

Figure 1. The black grid in the Brazil map indicates the region of interest for this study.

## 3. WRF MODEL

The version 2.2 of WRF model was used to simulate all the 38 days with higher number of CG flashes. The range of every run was 24 hours starting always at 00 UT of each day. The model was initialized using NCEP Global Forecast System (GFS) analysis. As illustrate in

Figure 2, the model setup included a coarse 30 km grid which extends from 32.424° to 14.141° S latitude and 62.426° to 33.574° W longitude and a nest 10 km grid resolution which extends by turn from 25.031° to 20.783° S latitude and 50.159° to 44.075° W longitude.

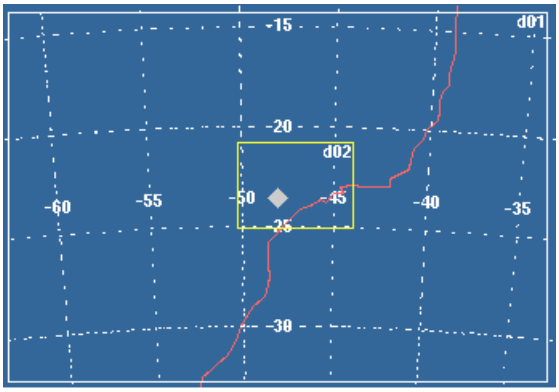

Figure 2. WRF domains: coarse domain (d01) of 30 km grid covering part of Brazil and Atlantic Ocean and nested domain (d02) of 10 km grid resolution covering almost all the São Paulo state.

As mentioned in the introduction, three different combinations of physics options were tested in the present study, exchanging the microphysics and cumulus parameterizations and keeping all the others the same. The microphysics includes explicitly resolved water vapor, cloud, hydrometeors distribution and precipitation processes. The model is general enough to accommodate any number of mass mixing-ratio variables, and other moments such as number concentrations. There are three layers in the atmosphere that are well defined by the models in terms of water phase: below the level of 0° C (presence of water vapor and water droplets), between 0° C and -40° C (presence of ice crystals and supercooled water droplets) and above the level of -40° C (only the presence of ice crystals and snow) (Skamarock et al., 2005). The main characteristics of the microphysics parameterizations used are following:

*WRF Single-Moment 3-class (WSM3) scheme* (Hong et al., 2004): includes ice sedimentation and other new ice-phase parameterizations. A major difference from other schemes is that a diagnostic relation is used for ice number concentration that is based on ice mass content rather than temperature. Three categories of hydrometeors are included: vapor, cloud water/ice and rain/snow.
*Eta Ferrier scheme* (Ferrier et al., 2002): predicts changes in water vapor and condensate in the forms of cloud water, rain, cloud ice, and precipitation ice (snow/graupel/sleet). The individual hydrometeor fields are combined into total condensate, and it is the water vapor and total condensate that are advected in the model.
*Purdue Lin scheme* (Lin et al. (1983) and Rutledge and Hobbs (1984)): includes six classes of hydrometeors: water vapor, cloud water, rain, cloud ice, snow and graupel.

Several techniques, called cumulus parameterizations, have been developed to estimate the subgrid scale effects of cumulus clouds in mesoscale models. These schemes are intended to represent vertical fluxes due to unresolved updrafts and downdrafts and compensating motion outside the clouds. They operate only on individual columns where the scheme is triggered and provide vertical heating and moistening profiles. Some schemes additionally provide cloud and precipitation field tendencies in the column and all of them provide the convective component of surface rainfall (Skamarock et al., 2005). Three cumulus schemes were chosen to be tested in the present work, as follows:

*Kain-Fritsch* (Kain, 2004): utilizes a simple cloud model with moist updrafts and downdrafts, including the effects of detrainment, entrainment and relatively simple microphysics.
*Betts-Miller-Janjic* (Janjic, 1994 and 2000): the deep convection profiles and the relaxation time are variable and depend on the cloud efficiency, a dimensionless parameter that characterizes the convective regime (Janjic, 1994). The shallow convection moisture profile is derived from the requirement that the entropy change is small and nonnegative (Janjic, 1994).
*Grell-Devenyi ensemble* (Grell and Devenyi, 2002): is an ensemble cumulus schemes in which effectively multiple cumulus schemes and variants are run within each grid box and then the results are averaged to give the feedback to the model. The schemes are all mass-flux type schemes but with differing updraft and downdraft entrainment and detrainment parameters and precipitation efficiencies. These differences in static control are combined with differences in

dynamic control, which is the method of determining cloud mass flux. The dynamic control closures are based on Convective Available Potential Energy (CAPE or cloud work function) or moisture convergence.

Regarding to other physics options in this study, it was used Rapid Radiative Transfer Model (RRTM) Longwave radiation (Mlawer et al., 1997) with the MM5 (Dudhia) Shortwave radiation scheme (Dudhia, 1989). The Similarity theory (MM5) scheme was used to simulate surface layer fluxes, whereas the Yonsei University (YSU) PBL scheme (Hong and Pan, 1996) was used to simulate boundary layer fluxes. The land surface fluxes were obtained with the Noah LSM (Chen and Dudhia, 2001).

The Table 1 summarizes the combinations of microphysics and cumulus parameterizations used with other physics options.

## 4. CASE STUDY: FEBRUARY 21, 2006

Skill scores are generally defined as measures of the relative accuracy of forecasts produced by two forecasting systems, one of which is a "reference system" (Murphy, 1988). The reference or truthful data used to verify a forecast generally comes from observational data. In many cases it is difficult to know the exact truth because there are errors in the observations. Sources of uncertainty include random and bias errors in the measurements themselves, sampling error and analysis error when the observational data are analyzed or otherwise altered to match the scale of the forecast. In most of the cases, the errors in the observational data are ignored since it is assumed that they are much smaller than the expected error in the forecast.

Table 1. Summary of the three WRF parameterizations sets used in this study. The expressions set 1, set 2 and set 3 will concern to their respective combinations in all the subsequent graphs.

| *WRF Physics Options* | ***Set 1*** | ***Set 2*** | ***Set 3*** |
|---|---|---|---|
| Microphysics | WSM3 | Eta Ferrier | Purdue Lin |
| Cumulus Parameterization | Kain-Fritsch | Betts-Miller-Janjic | Grell-Devenyi ensemble |
| Surface Layer | MM5 Similarity | MM5 Similarity | MM5 Similarity |
| Planetary Boundary Layer | YSU PBL | YSU PBL | YSU PBL |
| Land-Surface Model | Noah LSM | Noah LSM | Noah LSM |
| Atmospheric Radiation | RRTM/Dudhia | RRTM/Dudhia | RRTM/Dudhia |

Among the 38 days previously selected, February 21, 2006 was chosen because it provided the highest (11234) number of CG flashes from 17 to 21 UT. In order to evaluate the consistency of different variables from WRF model for this day, the bias or mean error will be calculated between the WRF forecasts and observational data, GFS analysis and Eta model forecasts, respectively.

If in a series of N forecasts, $F_i$ represents the i-th forecast and $O_i$ the corresponding observation or truthful value, the bias is given by:

$$BIAS = \frac{1}{N}\left[\sum_{i=1}^{N}(F_i - O_i)\right]$$

The bias indicates the average direction of the deviation from observed values, but may not reflect the magnitude of the error. A positive bias indicates that the forecast value exceeds the observed value on the average, while a negative bias corresponds to underforecasting the observed value on the average. Without comparative biases, there is no way to determine whether the forecast deviation is within acceptable limits and reflects the deviations occurring within the verification sample.

Firstly the WRF forecasts of 10 km grid generated from different sets of model parameterizations were compared with observational data from Companhia Ambiental do Estado de São Paulo (CETESB) and Centro de Previsão de Tempo e Estudos Climáticos (CPTEC) meteorological stations spread out along the domain (Figure 3). Air temperature and relative humidity at 2 m and wind magnitude at 10 m from WRF model were interpolated to the geographic coordinate of each meteorological station. The correspondence between the mean

forecasts and mean observations was calculated at 03, 06, 09, 12, 15, 18 and 21 LT. It was used local time intervals in order to show the variables behavior along the February 21st day.

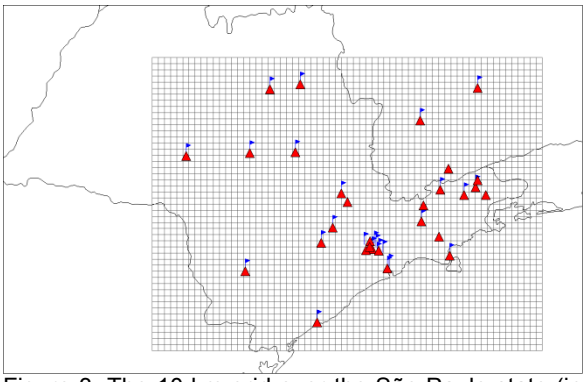

Figure 3. The 10 km grid over the São Paulo state (in Brazil southeastern) represents the nested domain used in WRF model. The red triangles indicate the location of 29 meteorological stations that provide 2m air temperature and relative humidity data. The blue barbs indicate the location of 27 meteorological stations that provide 10 m wind magnitude data.

All the bias results are displayed in Table 2 according to the parameterizations set used to run the WRF variables. In general it could be observed that the sets 1 and 2 presented on the average better responses in the simulations of 2 m air temperature and 10 m wind, respectively. At the beginning and end of these simulations for all the sets, the bias had its lowest values, what is unexpected considering that model errors are larger as it extends the integration time. The temperature was underestimated by the WRF model until 12 LT for all the sets, changing its tendency after that. The opposite behavior occurred with the wind. In the case of relative humidity, the forecasts from set 1 on the average better matched with the observed values, except at 15 LT when the variable was underestimated in almost 7%.

Another test done to check the consistency of WRF model for February 21st was to calculate the bias between mean forecasts 30 km grid and mean GFS analysis of 1 degree resolution to 3 synoptic hours: 06, 12 and 18 UT. This time range was chosen because of the availability of the GFS analysis every 6 hours. It will be analyzed only the forecasts from the WRF coarse domain due to the low resolution of the analysis. This comparison allows verifying the forecast behavior of basic variables like temperature and wind at low and medium levels from WRF model using different parameterizations sets in terms of altitude verification. The results are showed in Table 3. From all the sets, the temperature at 850 hPa is underestimated after 06 UT. The parameterizations of the set 2 on the average seem to better simulate the temperature at 850 and 500 hPa and the wind at 850 hPa. The lowest biases of the wind at 500 hPa were obtained with the set 3.

The last comparison involves forecasts of 20 km grid resolution from Eta model. The Eta model was installed at CPTEC in 1996 to complement the numerical weather prediction that has been held since early 1995 with the model of general atmospheric circulation (Chou, 1996). Its operational version at CPTEC is hydrostatic and covers most of South America and adjacent oceans. Currently the model is integrated 72 hours in the resolutions of 40 and 20 km with 38 vertical levels. Forecasts are given twice a day, with an initial condition at 00 and another at 12 UT. The initial condition comes from NCEP analysis and the lateral boundary conditions are derived from estimates of the CPTEC global model and updated every 6 hours. More details are given in Black (1994).

In Table 4 there are the biases calculated between mean WRF forecasts 10 km grid and mean Eta forecasts 20 km grid for temperature and wind at 850 and 500 hPa. The temperature in medium levels was better represented on the average by the set 3, except at 18 UT when the bias reached its highest value, more than 1.5° C. The wind at 850 and 500 hPa was overestimated by all the parameterizations sets, but the set 1 and 3 were that presented the lower biases for each case, respectively.

## 5. WRF MODEL *Vs* LIGHTNING

While the above analysis has been limited to just one case study, it allowed testing the WRF model and its consistency of forecast for one day with special weather conditions. As aforesaid, 38 days were selected for their significant amount of CG lightning during the afternoon between 17 to 21 UT, totalizing 107414 flashes. The main objective of this work is to run the WRF model to each day and parameterizations set in order to assess meteorological variables of interest in each lightning geographic coordinate.

Table 2. Comparisons between mean WRF forecasts 10 km grid and mean observational data.

| | BIAS | | | | | | | | |
|---|---|---|---|---|---|---|---|---|---|
| | 2m Air Temperature (°C) | | | 10 m Wind (m/s) | | | 2 m Relative Humidity (%) | | |
| Local Time | ***Set 1*** | ***Set 2*** | ***Set 3*** | ***Set 1*** | ***Set 2*** | ***Set 3*** | ***Set 1*** | ***Set 2*** | ***Set 3*** |
| 03 | -0.627 | -0.427 | -0.956 | 0.230 | 0.125 | 0.813 | -0.022 | -1.580 | 1.459 |
| 06 | -0.486 | -0.845 | -0.539 | 1.536 | 0.793 | 2.424 | -0.807 | -0.571 | -2.090 |
| 09 | -2.389 | -3.176 | -2.448 | 2.797 | 1.999 | 2.997 | -0.027 | 2.313 | 1.760 |
| 12 | -1.763 | -2.741 | -2.263 | 1.566 | 1.160 | 2.028 | 0.172 | 4.628 | 4.236 |
| 15 | 0.623 | 0.144 | -0.004 | -0.804 | -0.650 | -0.768 | -6.994 | -5.820 | -1.893 |
| 18 | 0.498 | 0.638 | 0.105 | -1.491 | -1.483 | -1.604 | -1.540 | -6.007 | 1.685 |
| 21 | 0.588 | 0.963 | 0.907 | -1.322 | -1.249 | -1.104 | -1.972 | -8.549 | 0.208 |

Table 3. Comparisons between mean WRF forecasts 30 km grid and mean GFS analysis.

| | BIAS | | | | | | | | | | | |
|---|---|---|---|---|---|---|---|---|---|---|---|---|
| | Temperature (°C) | | | | | | Wind (m/s) | | | | | |
| | 850 hPa | | | 500 hPa | | | 850 hPa | | | 500 hPa | | |
| UT Time | ***Set 1*** | ***Set 2*** | ***Set 3*** | ***Set 1*** | ***Set 2*** | ***Set 3*** | ***Set 1*** | ***Set 2*** | ***Set 3*** | ***Set 1*** | ***Set 2*** | ***Set 3*** |
| 06 | 0.021 | 0.030 | 0.059 | -0.036 | -0.137 | 0.217 | 0.148 | 0.057 | 0.116 | 0.057 | 0.104 | -0.059 |
| 12 | -0.352 | -0.283 | -0.300 | 0.360 | 0.267 | 0.498 | 0.460 | 0.273 | 0.570 | 0.063 | 0.188 | -0.051 |
| 18 | -0.230 | -0.177 | -0.383 | 0.414 | -0.043 | 0.770 | -0.046 | -0.369 | 0.301 | 0.151 | 0.406 | 0.096 |

Table 4. Comparisons between mean WRF forecasts 10 km grid and mean Eta forecasts 20 km grid.

| | BIAS | | | | | | | | | | | |
|---|---|---|---|---|---|---|---|---|---|---|---|---|
| | Temperature (°C) | | | | | | Wind (m/s) | | | | | |
| | 850 hPa | | | 500 hPa | | | 850 hPa | | | 500 hPa | | |
| UT Time | ***Set 1*** | ***Set 2*** | ***Set 3*** | ***Set 1*** | ***Set 2*** | ***Set 3*** | ***Set 1*** | ***Set 2*** | ***Set 3*** | ***Set 1*** | ***Set 2*** | ***Set 3*** |
| 06 | 0.457 | 0.246 | 0.520 | -0.285 | -0.266 | -0.121 | 1.731 | 1.738 | 1.833 | -0.285 | -0.266 | -0.121 |
| 12 | 0.294 | -0.102 | 0.130 | -0.652 | -0.853 | -0.234 | 1.332 | 0.181 | 2.305 | -0.652 | -0.853 | -0.234 |
| 18 | -0.572 | -1.115 | -1.062 | 0.718 | -0.587 | 1.637 | 0.105 | 0.870 | 0.403 | 0.718 | -0.587 | 1.637 |

CAPE, Lifted Index (LI), K-index (KI) and equivalent potential temperature (theta-e) were the meteorological variables chosen from WRF model 10 km grid to be interpolated to each lightning geographic coordinate. Many of these parameters or indices can be diagnosed from the observational radiosondes. Likewise, they can be forecasted from numerical weather output (Davis, 2001).

CAPE (Moncrieff and Green, 1972; Moncrieff and Miller, 1976) is the maximum energy available to an ascending parcel, according to the parcel theory. On a thermodynamic diagram, this is called positive area, and can be seen as the region between the lifted parcel process curve and the environmental sounding, from the parcel's level of free convection to its level of equilibrium. According to Nascimento (2005), in general values of CAPE from 1000 to 2500 J/kg are considered high, values above 2500 J/kg show strong instability, and above 4000 J/kg indicate extreme instability.

The LI (Galway, 1956) is calculated as the difference between the observed temperature at 500 hPa and the temperature of an air parcel lifted to 500 hPa from near the surface. The more unstable the environment, more negative the LI. According to Yair et al. (2010), the LI values and the risk of thunderstorms and severe weather activity are: LI > 2, no significant activity; 0 < LI < 2, showers/thunderstorms possible (additional lift needed); -2 < LI < 0, thunderstorms possible; -4 < LI < -2, thunderstorms more probable, but few, if any severe; and LI < -4, severe thunderstorms possible.

The K index (Sturtevant, 1995) is a useful tool for diagnosing the potential for convection. Its computation takes into account the vertical distribution of both moisture and temperature. It does not require a skew-T diagram; it is simply

computed from air temperatures at 850, 700, and 500 hPa, and dew point temperatures at 850 and 700 hPa. The thunderstorm potential based on the critical values of KI, according to Sturtevant (1995), defines the probability in percentage for occurrence. The thunderstorm potential for the different values of KI is as follows: 0% for KI = 0-15; 20% or unlikely for KI = 18-19; a 35% potential or an isolated thunderstorm, for KI = 20-25; 50% potential or widely scattered thunderstorms for KI = 26-29; 85% potential or numerous thunderstorms for KI = 30-35; and 100% (certain) chance for thunderstorms for KI values > 36.

Theta-e is the temperature a sample of air would have if all its moisture were condensed out by a pseudo-adiabatic process and the sample then brought dry-adiabatically back to 1000 hPa (Bolton, 1980). The increase in theta-e implies greater instability of the atmosphere. Values of theta-e at surface in moist environments that support deep convection are about 330K.

The results of this analysis are presented as histograms of lightning occurrence in Figure 4. There is a histogram for each variable simulated in WRF model using the 3 sets of parameterizations. The positive x-axis indicates an increase in the critical values of all the variables with respect to instability. The value ranges can be checked in Table 5.

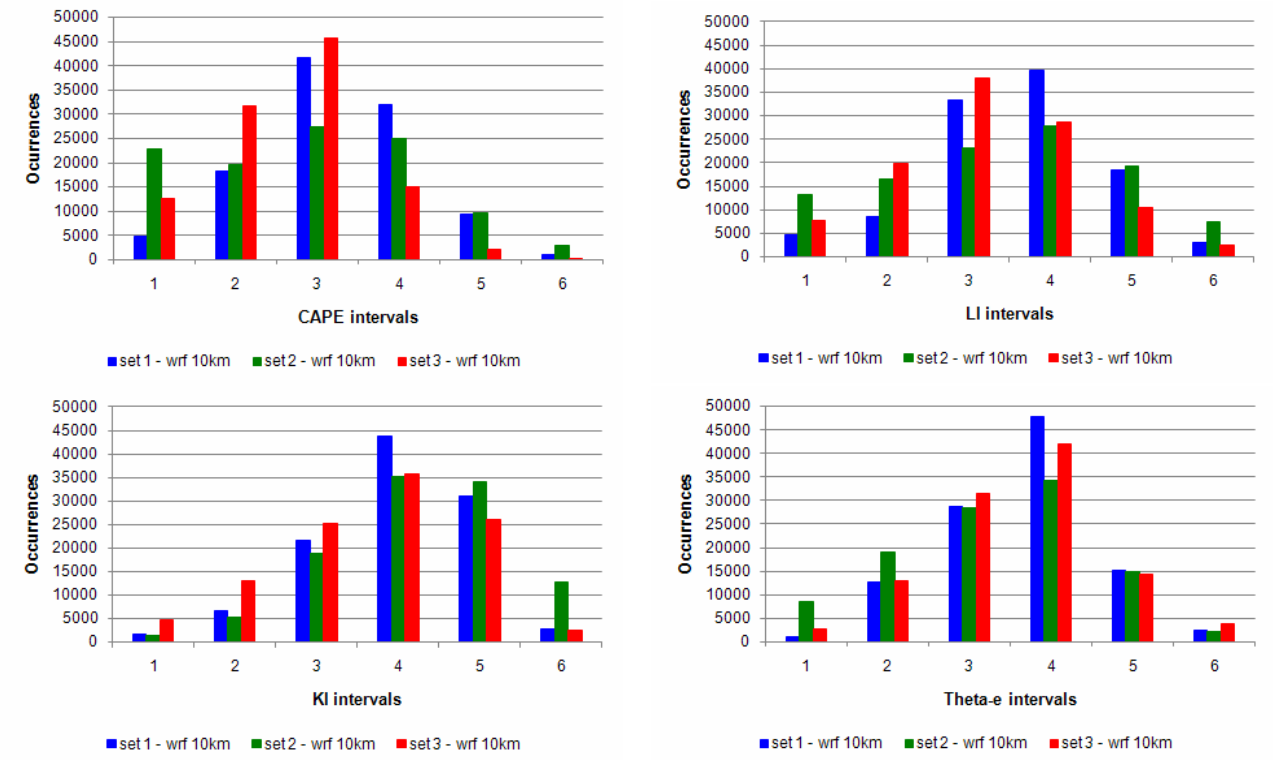


Figure 4. Histograms of lightning occurrence to CAPE, LI, KI and theta-e simulated in WRF model using 3 different sets of parameterizations. The x-axis indicates intervals of values for each variable, which were determined observing the maximum and minimum interpolated value. The Table 5 shows the designation of the intervals.

Analyzing Table 5, it is important to note that independently of the parameterizations set used the WRF model showed a good performance in the simulation of the meteorological variables for days with lightning, since their values are consistent with those previously found in thunderstorm studies. In general the interval 4 has the largest frequency of lightning, except for CAPE. Looking at the lightning distribution along the values range, the sets 1 and 2 seem to better represent all the variables. Table 6 presents the skill score of each parameterizations set. The percentages were calculated summing all the lightning occurrences

of the last four intervals and dividing it by the total. The set 1 presented the best score for CAPE, LI, and theta-e and almost to KI by a difference of 2% compared to set 2.

Table 5. Value ranges of the meteorological variables in the histograms of the Figure 4.

| *Intervals* | RANGES | | | |
|---|---|---|---|---|
| | CAPE (J/kg) | LI ($^{o}$C) | KI ($^{o}$C) | Theta-e (K) |
| 1 | < 500 | > (-1) | < 28 | < 345 |
| 2 | 500 – 1000 | (-1) – (-2) | 28 – 31 | 345 – 350 |
| 3 | 1000 – 1500 | (-2) – (-3) | 31 – 34 | 350 – 355 |
| 4 | 1500 – 2000 | (-3) – (-4) | 34 – 37 | 355 – 360 |
| 5 | 2000 – 2500 | (-4) – (-5) | 37 – 40 | 360 – 365 |
| 6 | > 2500 | < (-5) | > 40 | > 365 |

Table 6. Skill score of the parameterizations sets.

| *Parameterizations Set* | SKILL SCORE | | | |
|---|---|---|---|---|
| | CAPE | LI | KI | Theta-e |
| Set 1 | 78% | 88% | 92% | 87% |
| Set 2 | 60% | 72% | 94% | 75% |
| Set 3 | 59% | 74% | 83% | 85% |

## 6. CONCLUSIONS

In this work it was proposed a method to identify which is the combination of parameterizations in WRF model that better represents the atmospheric conditions when lightning occurs in the Brazil southeastern. Some comparisons between WRF forecasts and reference data was done in order to check the consistency and quality of WRF model for the day with the highest number of CG lightning flashes from the whole study period. This first analysis allowed verifying that in general the sets of parameterizations 1 and 2 better represented temperature and wind at surface, low and medium levels in the atmosphere. The next step in this study was to identify four WRF variables that are related to atmospheric instability and interpolate them to the geographic coordinates of more than 100000 lightning. Although the sets 1 and 2 have been highlighted again among all the combinations, the set 1 was the one which presented the best results for the meteorological variables.

This evaluation method might be used in the future for a lighting forecast algorithm, once the identification of favorable meteorological conditions to predict lightning occurrence is essential to provide reliable warnings and anticipate precaution measures that minimizes the negative impact of this phenomenon.

## 7. REFERENCES


Black, T. L., 1994: The new NMC Mesoscale Eta Model: Description and Forecast examples. *Wea. Forecasting*, **9**, 265-278.

Bolton, D., 1980: The computation of equivalent potential temperature. *Mon. Weather Rev.*, **108**, 1046-1053.

Chen, F.; Dudhia, J., 2001: Coupling an advanced land-surface/ hydrology model with the Penn State/ NCAR MM5 modeling system. Part I: Model description and implementation. *Mon. Wea. Rev.*, **129**, 569–585.

Chou, S. C., 1996: Modelo Regional Eta. Climanálise Especial 10 anos, 11, n. especial. Available at: (http://climanalise.cptec.inpe.br/~rclimanl/boletim/cliesp10a/27.html).

Davis, R. S., 2001: Flash flood forecast and detection methods in Severe Convective Storms. *Meteorol. Monogr.,* vol. 50, pp. 481–525, Am. Meteorol. Soc., Boston, Mass.

Dudhia, J., 1989: Numerical study of convection observed during the winter monsoon experiment using a mesoscale two-dimensional model, *J. Atmos. Sci.*, **46**, 3077–3107.

Ferrier, B. S.; Jin, Y.; Lin, Y.; Black, T.; Rogers, E.; DiMego, G., 2002: Implementation of a new grid-scale cloud and precipitation scheme in the NCEP Eta model. Preprints

15th Conf. on Numerical Weather Prediction, San Antonio, TX, *Amer. Meteor. Soc*., 280–283.

Galway, J. G., 1956: The lifted index as a predictor of latent instability. *Bull. Amer. Meteor. Soc.*, 43, 528-529.

Grell, G. A.; Dévényi, D., 2002: A generalized approach to parameterizing convection combining ensemble and data assimilation techniques. *Geophys. Res. Lett.*, **29** (14), 1693, doi: 10.1029/2002GL015311.

Hong, S.Y., J. Dudhia, and S.H. Chen, 2004: A Revised Approach to Ice Microphysical Processes for the Bulk Parameterization of Clouds and Precipitation. *Mon. Wea. Rev.*, **132**, 103–120.

Hong, S. Y.; Pan, H. L., 1996: Nonlocal boundary layer vertical diffusion in a medium-range forecast model, *Mon. Wea. Rev.*, **124**, 2322–2339.

Iribarne, J. V.; Cho, H. R., 1980: *Atmospheric Physics*. Dordrecht: D. Reidel Publishing Company, 212 p. 77734 cm. ISBN 90-277-1033-3.

Janjić, Z.I., 1994: The Step-Mountain Eta Coordinate Model: Further Developments of the Convection, Viscous Sublayer, and Turbulence Closure Schemes. *Mon. Wea. Rev.*, **122**, 927–945.

Janjić, Z. I., 2000: Comments on "Development and Evaluation of a Convection Scheme for Use in Climate Models". *J. Atmos. Sci.*, **57**, 3686.

Kain, J. S., 2004: The Kain–Fritsch Convective Parameterization: An Update. *J. Appl. Meteor.*, **43**, 170–181.

Lin, Y. L.; Farley, R. D.; Orville, H. D., 1983: Bulk Parameterization of the Snow Field in a Cloud Model. *J. Appl. Meteor.*, **22**, 1065–1092.

Mlawer, E. J.; Taubman, S. J.; Brown, P. D.; Iacono, M. J.; Clough, S. A., 1997: Radiative transfer for inhomogeneous atmosphere: RRTM, a validated correlated-k model for the longwave. *J. Geophys. Res.*, **102** (D14), 16663–16682.

Moncrieff, M. W.; Green, J. S. A., 1972: The propagation of steady convective overturning in shear. *Quart. J. R. Met. Soc.*, **98**, 336-352.

Moncrieff, M. W.; Miller M. J., 1976: The dynamics and simulation of tropical cumulonimbus and squall lines. *Quart. J. R. Met. Soc.*, **102**, 373-394.

Murphy, A. H., 1988: Skill scores based on the mean square error and their relationships to the correlation coefficient. *Mon. Wea. Rev.*, **116**, 2417-2424.

Naccarato, K. P., 2006: *Análise das Características dos Relâmpagos na Região Sudeste do Brasil*. 362 p. (INPE-14083-TDI/1069). Tese (Doutorado em Geofísica Espacial) – INPE, São José dos Campos.

Nascimento, E. L., 2005: Previsão de tempestades severas utilizando-se parâmetros convectivos e modelos de mesoescala: uma estratégia operacional adotável no Brasil? *Revista Brasileira de Meteorologia*, 20, 1, 121-140.

Pinto Jr., O.; Naccarato, K. P.; Pinto, I. R. C. A.; Fernandes, W. A.; Neto, O. P., 2006: Monthly distribution of cloud-to-ground lightning flashes as observed by lightning location systems. *Geophys. Res. Lett.*, **33**, L09811, doi: 10.1029/2006GL026081.

Ruiz, J. J.; Ferreira, L.; Saulo, A. C., 2007: WRF-ARW sensitivity to different planetary boundary layer parameterization over South America. 4-11, 4-12 Research activities in atmospheric and oceanic modeling. WGNE blue book, WMO available at: (http://collaboration.cmc.ec.gc.ca/science/wgne/BlueBook/index.html).

Ruiz, J. J.; Saulo, A. C., 2006. Quantitative precipitation forecast verification over southeastern South America using CMORPH and CPC Data. 5-47, 5-48 Research activities in atmospheric and oceanic modeling. WGNE blue book, WMO available at: (http://collaboration.cmc.ec.gc.ca/science/wgne/index.html).

Ruiz, J. J.; Saulo, A. C.; Nogues-Paegle, J. 2009: Sensibilidad del pronóstico de variables de superficie a la utilización de diferentes parametrizaciones en el modelo WRF: ¿Es posible encontrar la mejor configuración? *Actas del X Congreso Argentino de Meteorología*, XIII Congreso Latinoamericano e Ibérico de Meteorología, Buenos Aires, Argentina. 21 p.

Rutledge, S. A.; Hobbs, P. V., 1984: The mesoscale and microscale structure and organization of clouds and precipitation in midlatitude cyclones. XII: A diagnostic modeling study of precipitation development in narrow cloud-frontal rainbands. *J. Atmos. Sci.*, **41**, 2949–2972.

Skamarock, W. C.; Klemp, J. B.; Dudhia, J.; Gill, D. O.; Barker, D. M.; Wang, W.; Powers, J. G., 2005: A description of the advanced research WRF Version 2. *NCAR Tech. Notes*. Natl. Cent. for Atmos. Res., Boulder, Colorado.

Silva Junior, R. S., 2009: *Sensibilidade na estimativa da concentração de poluentes fotoquímicos com a aplicação de diferentes parametrizações da Camada Limite Planetária utilizando o modelo de qualidade do ar WRF/Chem*. 171 p. Tese (Doutorado em Meteorologia) – Universidade de São Paulo, São Paulo.

Stanski, H. R.; Wilson, L. J.; Burrows, W. R., 1989: Survey of common verification methods in meteorology. *World Weather Watch Tech. Rept.* N$^{o}$ 8, WMO/TD N$^{o}$ 358, WMO, Geneva, 114 p.

Sturtevant, J. S., 1995: *The Severe Local Storm Forecasting Primer*. 197 pp., Weather Scratch Meteorol. Serv., Florence, Ala.

Yair, Y.; Lynn, B.; Price, C.; Kotroni, V.; Lagouvardos, K.; Morin, E.; Mugnai, A.; Llasat, M. d. C., 2010: Predicting the potential for lightning activity in Mediterranean storms based on the Weather Research and Forecasting (WRF) model dynamic and microphysical fields. *J. Geophys. Res.*, **115**, D04205, doi: 10.1029/2008JD010868.